Detection of Intelligent Tampering in Wireless Electrocardiogram Signals Using Hybrid Machine Learning

Siddhant Deshpande, Yalemzerf Getnet ⬤, Waltenegus Dargie ⬤, *Senior Member, IEEE*

Abstract—**With the proliferation of wireless electrocardiogram (ECG) systems for health monitoring and authentication, protecting signal integrity against tampering is becoming increasingly important. This paper analyzes the performance of CNN, ResNet, and hybrid (Transformer+CNN) models for tamper detection. It also evaluates the performance of a Siamese network for ECG-based identity verification. Six tampering strategies, including structured segment substitutions and random insertions, are emulated to mimic real-world attacks. The one-dimensional ECG signals are transformed into a two-dimensional representation in the time-frequency domain using the continuous wavelet transform (CWT). The models are trained and evaluated using ECG data from 54 subjects recorded in four sessions (2019–2025) outside of clinical settings while the subjects performed seven different daily activities. Experimental results show that in highly fragmented manipulation scenarios, CNN, FeatCNN-TranCNN, FeatCNN-Tran and ResNet models achieved an accuracy exceeding 99.5%. Similarly, for subtle manipulations (e.g., 50%–50%) and (75%–25%) substitutions, our FeatCNN-TranCNN model demonstrated consistently reliable performance, achieving an average accuracy of 98%. For identity verification, the pure Transformer-Siamese network achieved an average accuracy of 98.30%. In contrast, the hybrid CNN+Transformer-Siamese model delivered perfect verification performance with 100% accuracy.**

Index Terms—**Continuous Wavelet Transform (CWT), Convolutional Neural Network (CNN), ECG signal, Tampering, Transformers**

I. INTRODUCTION

Electrocardiogram (ECG) signals have played an important role in the diagnosis and monitoring of cardiovascular diseases [1], [2]. As interest in preventive medicine grows, wireless ECG signals are being used for continuous health monitoring and biometric authentication [3]–[5]. However, wireless ECG data is vulnerable to different kinds of attacks [6], [7]. An ECG signal can be manipulated by replacing some part of ECG segment, or it can be manipulated by replacing the whole part of the ECG segment with another person's ECG segment. Also, the manipulation can be conducted by using artificially generated ECG signals, and all these manipulations can affect the integrity of biometric systems [8], [9]. Several studies have been conducted to detect tampering or anomalies in ECG

signals, ranging from traditional methods to machine learning-based systems [10]. Traditional methods identify manipulations, but they face scalability issues and struggle to identify complex attack strategies [11]–[13]. Conventional machine learning approaches, such as Support Vector Machines (SVMs) and Random Forests, have better performance compared to traditional methods [14]–[16]. However, these methods rely on manually created features, and because of this, they are less adaptive to unknown and more complicated attacks. Deep learning models, such as feed-forward networks and convolutional neural networks (CNNs), have been used to identify ECG signal manipulation, but they are not evaluated with sophisticated manipulation techniques [17]–[20]. Likewise, Siamese Neural Networks [21]–[23] are employed for person-specific verification, relying on individual ECG features to improve robustness between subject variability.

In this paper, a comprehensive deep learning framework used for tampering detection as well as biometric identification is presented. The performance of different deep learning models, such as CNNs, ResNet, Transformer models, and hybrid models (Transformer+CNNs) are investigated under several tampering scenarios. In addition to this, the performance of a Siamese neural network in biometric verification is evaluated. The experiments are conducted on a multi-session ECG dataset of 54 subjects, and the results show that a ResNet model and a hybrid CNN-Transformer model achieved high accuracy in tamper detection and a hybrid CNN-Transformer model achieved high accuracy in identity verification. The accuracy of CNN and ResNet models is high in detecting highly localized tampering; however, the training results show that these models highly depend on specific training parameters. The hybrid Transformer-CNN based models achieved high accuracy as well as a high degree of stability and consistent training results. The study conducted highlights that the hybrid Transformer-CNN model is more effective at securing wireless ECG signals, thus improving the reliability of remote medical monitoring and biometric authentication. The contributions of this paper are summarized as follows:

- **Data:** Our approach is real-world data-driven. A large volume of ECG data was collected from 54 subjects carrying out 7 different activities. The data were collected in four batches between 2019 and 2025 and exhibit a high variance, both across subjects and across activities.
- **Model for recognizing tampering:** Multiple machine learning frameworks such as CNN, ResNet, and hy-

brid models were proposed for tampering detection, and Siamese Neural Networks are proposed for robust identity verification. All these models were evaluated against different tampering strategies, and the performance of each model is compared with the others.

- **Experiments:** Extensive and independent experiments were conducted, and the results show that the proposed models are effective in identifying complex ECG tampering. Specifically, hybrid models achieved high performance in tamper detection against various tampering attacks on wireless ECG data. Also, Siamese Networks achieved accuracy of more than 99% in person verification.

The remainder of this paper is organized as follows. Section II provides a review of related work in the field. Section III describes the data acquisition process. In Section IV, we outline the strategies used for feature identification and extraction. Section V details the proposed model architecture, including parameter selection and configuration. Section VI presents the evaluation methodology along with quantitative results. Finally, Section VII, offers concluding remarks and discusses potential directions for future research.

II. RELATED WORK

The widespread use of wireless ECG data for healthcare monitoring and person identity verification has led to concern about the wireless ECG data's authenticity. Various ECG data tampering detection mechanisms are proposed to improve the reliability of wireless ECG data, and the proposed approaches are discussed in this section.

In [24], the authors proposed a Quantum Arrhythmia Detection System (QADS). The system developed secure ECG data by using quantum blockchain technology, which uses a blockchain algorithm that integrates a controlled quantum walk hash function and a quantum authentication protocol during block creation. To detect irregular heartbeats, temporal features are extracted from securely stored ECG data by using a hybrid quantum convolutional neural network (HQCNN). The method is tested on the MIT-BIH Arrhythmia database, and HQCNN achieved an accuracy of 94.3% and CNN achieved an accuracy of 92.5%.

Manipulatable Haar Transform (MHT) technique, a non-invertible transformation technique, is developed in [25]. The method is used to identify individuals based on ECG data, and it is also used to protect wireless ECG data against potential threats. A stable temporal feature vector is first extracted from the ECG signal collected. Then, the MHT is performed on the extracted ECG feature vector to convert it to another version in a noninvertible manner. This conceals the sensitive information contained in the extracted feature vector. A second feature vector extracted synchronically from the same user by another sensor node is transformed in the same way as the first feature vector. Finally, authentication takes place in the encrypted domain by comparing the transformed versions of the two feature vectors. The simulation result tested on PTB dataset show that an equal error rate (EER) 7.62% is achieved.

A study in [26] proposed dual-attention W-Net (a DAW-Net), a dual-attention-based dual encoder-decoder architecture

designed to separate maternal (mECG) and fetal (fECG) signals from abdominal ECG (aECG) signals affected by noise from diverse sources. The network extracts feature maps related to both maternal and fetal QRS complexes, enabling separation of mECG and fECG signals. Correlation attention enhances fetal QRS by masking relevant regions, while self-attention captures maternal QRS context for removal, and skip connections amplify QRS signal clarity. The model was evaluated using two real datasets, FECGSYNDB[1] and ABFECGDB[2], and obtained F1 score of 98.13%.

CNN and self-supervised contrastive learning were developed in [27] to extract user-specific features from unlabeled ECG data. CNN was trained on large, unlabeled datasets by using contrastive learning, and this learning method is used to improve model generalization. The model is tested using MIT-BIH and ECG-ID datasets and achieved 99.15% accuracy.

The study in [11] proposed the Statistical N-best Adaptive Fourier Decomposition (SAFD), a method that extends the traditional n-best Adaptive Fourier Decomposition (AFD) [28] from single-signal to multi-signal processing and operates within the stochastic Hardy space. The SAFD method learns some atoms that effectively capture the internal structure of ECG signals and can produce a discriminative representation that preserves their time-frequency characteristics. The model is used for biometric identification, and it is evaluated on five ECG databases (Fantasia, MITDB, ECG-ID, EDB, and AED) to achieve an accuracy of 97.59%.

The Singular Value Decomposition (SVD) method was proposed in [29], and the proposed method was applied to denoise the ECG signals by extracting orthonormal eigenvectors that capture essential features and separate orthogonal components. To validate the method, a study was conducted involving human subjects under varying exercise levels. ECG signals are acquired via a wearable module and transmitted wirelessly to a processing device, then Singular Value Decomposition (SVD) is applied to denoise the signals. Extracted features are stored both locally and in the hospital database. During authentication, new ECG and motion data are collected, motion is detected, and the ECG is adaptively denoised then it is compared with stored ECG signal. An accuracy rate of about 90% was achieved when the model was tested on the MIT-BIH Arrhythmia (MA) database and the MIT-BIH Noise Stress Test (NST) database.

In [30], a 1D-CNN model is proposed for identifying and classifying multiple simultaneous contaminants in sEMG signals without prior feature extraction. The model was evaluated using data collected from five subjects under five different contamination scenarios: ECG+MA+PL[3], ECG+AS+AWGN, ECG+MA[4]+AWGN, ECG+PL+AWGN, and PL+AS+AWGN[5]. In all cases, the model achieved an accuracy exceeding 85%.

The multi-layer Convolutional Neural Network (CNN) was proposed in [31] for wireless ECG signals and motion sensors

---

[1]https://physionet.org/content/fecgsyndb/1.0.0/sub01/
[2]https://www.physionet.org/content/adfecgdb/1.0.0/
[3]Power Line noise
[4]Motion Artifacts
[5]Additive White Gaussian Noise

based biometric identification. Time and frequency domain features were extracted and used to train the proposed model. The model was tested using data collected from a total of 34 participants who performed seven distinct activities while their physiological and motion data were recorded. The model obtain over 98% classification accuracy, with 85% of participants being identified with 100% accuracy. Additionally, the model recognized the performed activities with an average accuracy of 92%.

The proposed approaches demonstrate reliable detection of complex signal manipulations. However, most of these approaches account for external manipulations. In contrast, the present work does not rule out internal manipulation, i.e., the deliberate manipulation of ECG data by users to achieve various goals, such as concealing heart conditions and making insurance claims. In contrast to the data used in previous case studies, which were collected in controlled environments, the present work used data collected outside of clinical settings during various activities by subjects. Such data are difficult to evaluate and contain significant motion artifacts. The robust machine learning models we propose ensure that these challenges are successfully overcome.

III. DATA ACQUISITION

We employed the Shimmer platform (version 3)[6] to measure cardiac and physical activities. The platform avails 5 ECG channels, all of which were sampled synchronously at a rate of 512 samples per second. The measurements were taken in four separate batches of experiments. The first batch took place in 2019, with 8 healthy subjects (all males, mean age = 30 yrs, SD = 6 yrs) performing 7 different activities (sitting, standing, bending over, climbing up and down a staircase, jumping on the spot, walking, and running). Each activity lasted 120 s. The second and the third batches took place in 2024. The second batch consisted of 16 subjects, 11 of which were females and 5, males. For this batch, the mean age = 27 yrs and SD = 13 yrs. Thirteen of the subjects were healthy; one of them had asthma, another took regular medication which could affect blood pressure; and one of them, a 27 years old female, was a smoker. The third batch consisted of 10 healthy subjects, five females and 5 males, all between 21 and 24 years of age. The mean age was 22 yrs and SD = 1.9 yrs. The fourth batch took place in 2025 and consisted of 20 subjects. The average age in this batch is 24.2 with a SD = 2.26 yrs.

All data were collected with the permission of the TU Dresden's Ethic Committee (under Application No. EK271072017). Full consent from all participants had been obtained prior to the experiments.

TABLE I: Summary of All Batches

Batch (Year)	Number of Participants	Male/Female Ratio (M/F)	Mean Age ± SD
2019	8	8/0	30 ± 6 years
2024	16	5/11	27 ± 13 years
2024	10	5/5	22 ± 1.9 years
2025	20	17/3	24.2±2.26 years

[6]https://shimmersensing.com/product/consensys-ecg-development-kits/.

IV. FEATURES

Preprocessing of the ECG signal is conducted to extract features effectively by removing artifacts, reducing noise, and standardizing inputs. The pre-processing pipeline includes signal segmentation, band-pass filtering, normalization, and transformation input into the time-frequency domain.

A. Segmentation

The raw ECG signals is segmented into fixed-length frames of 4 seconds (corresponding to 2048 samples at a 512 Hz sampling rate), with a 30% overlap between consecutive segments. Segments shorter than 4 seconds were excluded from further processing. The 30% overlap is chosen to enhance the detection of tampering patterns that occur near segment boundaries while avoiding excessive data redundancy and computational overhead. To have sufficient information from ECG signal for robust wave form analysis and maintaining a manageable input size, a 4-second segment length was selected. Segments shorter than this risk omitting critical signal features, whereas segment longer than these windows may increase computational demands and dilute the localized detection of tampering artifacts.

B. Filtering

The raw ECG signals are contaminated with various types of noise, including baseline wander due to respiration, power line interference at 50/60 Hz, and high-frequency noise originating from muscle activity. A band-pass second-order Butterworth filter with cutoff frequencies set at 0.5 Hz and 100 Hz is used to effectively attenuate noise while preserving clinically relevant cardiac signal feature. This frequency was selected since frequencies below 0.5 Hz typically correspond to baseline drift caused by respiration and electrode motion, whereas frequencies above 100 Hz are frequencies of muscle artifacts and external interference.

C. Min-Max Normalization

After conducting the filtering process , Min-Max normalization is applied to each ECG segment, except the segments used for the identity verification task, the segment in the identity verification task is not normalized in order to preserve the original morphological differences between subjects.

To ensure that tampered regions appeared subtle and visually indistinct, particularly at the transition points between authentic and manipulated segments, each segment was independently normalized to a [0, 1] range. In scenarios involving partial tampering, signal segments from different sources may exhibit varying baseline offsets or amplitude scales and can create detectable transitions if the ECG signal is not normalized properly.
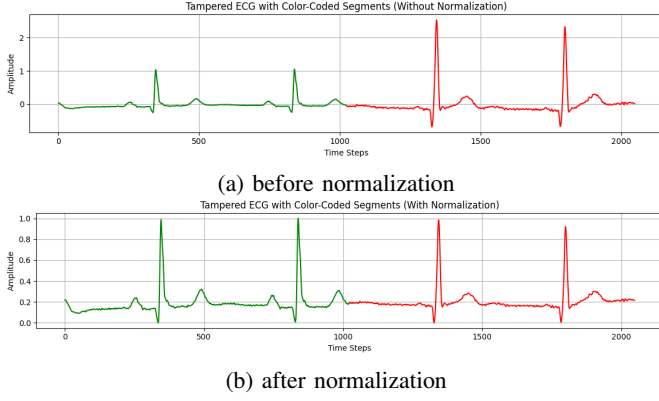
(a) before normalization

(b) after normalization

Fig. 1: Tampering before and after normalization

D. Continuous Wavelet Transform (CWT)

The scalograms that captured both temporal and spectral characteristics of the ECG signals are generated by using the Continuous Wavelet Transform (CWT) method, a method used to transform the one-dimensional ECG time-series signals into two-dimensional time-frequency signals. Each segment produced a transformed output of shape (2048, 96), where 2048 corresponds to time samples and 96 to frequency bins. The choice of 96 scales provided a balance between resolution and computational efficiency. These generated scalograms served as inputs for the hybrid model (transformer-CNN), and the original preprocessed 1D ECG signals were used as an input for the CNN and ResNet models. The hybrid model used the generated input signal, since it is difficult to extract localized frequency variations from the raw time-domain ECG signal.

E. Tampering ECG Signal

There are two types of tampering, the first one is partial segment tampering, a tampering mechanism where some segments span the boundary between original and injected data. The second one is a full segment replacement tampering mechanism, where the entire segments fall within tampered regions and appear structurally coherent, resembling genuine ECG signs. These two tampering mechanisms have distinct characteristics, and therefore it is difficult to detect both tampering scenarios effectively by using a single method. To address this challenge, two detection strategies are proposed: Transformer, CNN, ResNet and Transformer-CNN hybrid models are trained to identify structural anomalies linked to partial tampering. For identity verification (full segment replacement), a Siamese neural network was used to verify the identity associated with each segment. In this paper, to evaluate the performance of the model proposed, different types of tampering ECG signals are generated artificially, and also various partial tampering techniques were designed with differing levels of complexity and subtlety. All manipulation methods are applied at the segment level, with each ECG segment spanning 4 seconds (2048 samples at a 512 Hz sampling rate). Each tampering scenario was formed by merging an ECG segment from one person (person A) with other individual (person B). The ECG segments are recorded from each person

when they are doing the same physical activity; this activity-aware pairing strategy is adopted to avoid bias of the model toward detecting changes in activity rather than actual signal level inconsistencies indicative of tampering. Six tampering scenarios were simulated by using the blending method.
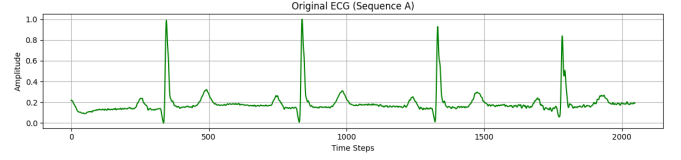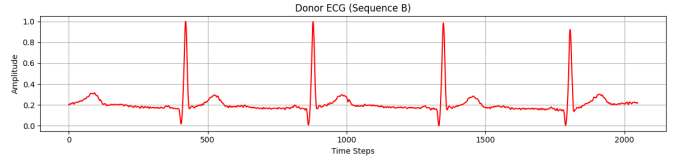

Fig. 2: Original ECG from Person A

Fig. 3: Donor ECG from Person B

Blending Process: Linear blending method is proposed to achieve a smooth transition between the end of the preceding segment and the beginning of the subsequent one, it is used to ensure a gradual transition by weighting signal values across a fixed blending window (e.g., 5 samples), thereby reducing the visibility of abrupt amplitude or phase changes that could reveal tampering artifacts.

$$\text{blended} = (1 - \alpha) \cdot \text{prev\_tail} + \alpha \cdot \text{curr\_head}$$

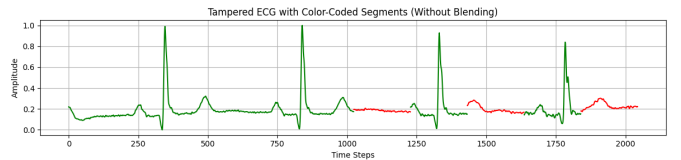Where α is a linearly spaced vector from 0 to 1 across the blending width.

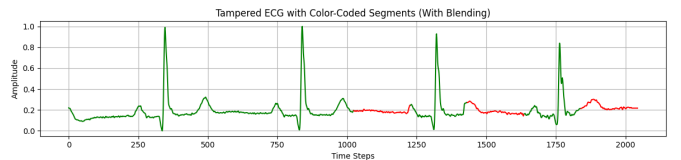Fig. 4: Tampered ECG segment without linear blending.

Fig. 5: Tampered ECG segment with linear blending.

1) 50-50 Replacement: In this tampering scenario, 50% of the ECG segment is from person A, and the remaining 50% is from person B. This tampering mechanism is one of the simplest tampering mechanisms, but the use of linear blending for merging the two ECG signals at the midpoint makes it difficult to be detected.
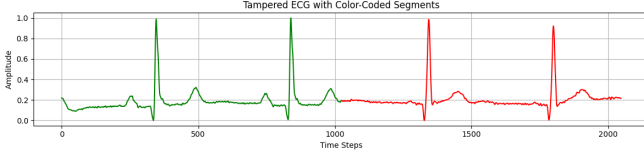
Fig. 6: Tampered ECG: First half from Person A (green), second half from Person B (red)

2) 75-25 Asymmetric Tampering (A-B): This tampering strategy keeps 75% of the segment from Person A and substitutes the last 25% with Person B's signal. The goal is to produce a more subtle tampering that influences a trailing part of the segment. The segment boundary is close to the end, and because of blending, it is hard to see and to detect algorithmically.
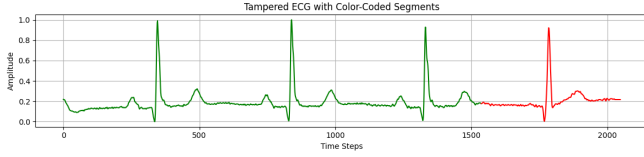

Fig. 7: Tampered ECG: 75% from A, 25% from B

3) 50-25-25 Multi-Source Replacement (A-B-A): This tampering mechanism used a three part composition, where the first 50% of the signal is from Person A, 25% from Person B and the remaining 25% from Person A.
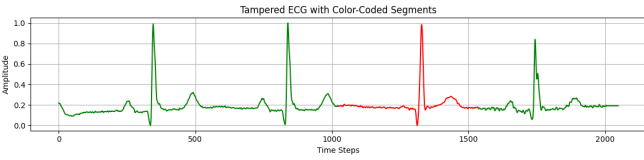

Fig. 8: Tampered ECG: A-B-A pattern, with colour-coded segments

4) Alternating Blend Pattern (50-10-10-10-10-10): This tampering method was highly structured, where the attacker attempts to make the data look more natural by constantly alternating the ECG signals From person A and person B. The combination mechanism used in this tampering was the first half was from Person A, 10% from B, and then 10% from A, and for the remaining 30% it switches between A and B. This type of tampering is rhythmic tampering, which is challenging to detect visually because of quick transitions and uniform blending at every transition.
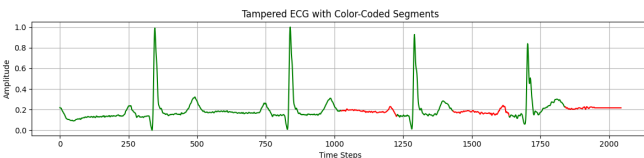

Fig. 9: Tampered ECG: Alternating blend of Person A and B (color-coded)

5) Sporadic 20% Replacement: In this tampering method, 20% of the total ECG segment is substituted by several short, non-contiguous donor fragments of equal size. In particular, four segments, each accounting for 5% of the total length of the sequence, are placed at random locations in the 4-second signal. No large contiguous area is entirely from Person B, making the tampering subtle and hard to notice visually or statistically.
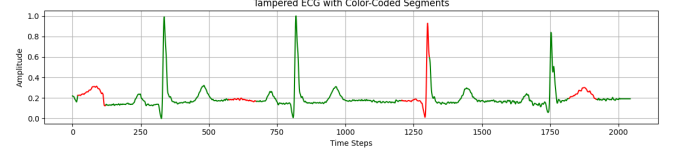

Fig. 10: Tampered ECG: Sporadic insertions from Person B (red) into Person A's signal (green)

6) Sporadic 50% Replacement: This strategy expands the 20% variant by raising the tampered part to 50% of the signal. The segment is interrupted by ten donor fragments, each of which make up 5% of the ECG. The fact that this tampering is common, but granular, might present a unique challenge to detection models, because the changes are subtle, but pervasive across a large amount of the data.
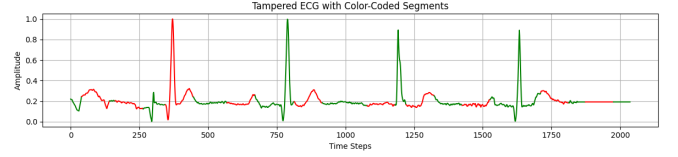

Fig. 11: Tampered ECG: Roughly half of the segment replaced with donor signal (red)

V. MODEL

This section outlines the deep learning models we developed for tampering detection and person identification. The models developed for tampering detection identify signal irregularities that indicate manipulation, and the models for individual identification determine whether a given segment belongs to a particular individual.

A. Model Architectures for Partial Tampering Detection

1) CNN Model: The CNN model developed detects tampering artifacts from one-dimensional ECG signals by extracting short and localized temporal patterns like QRS complexes, P-wave disruptions and small frequency abnormalities, which are important tampering indicators in ECG signals.

The model proposed is constructed from 3 Conv1D layers followed by batch normalization, dropout and max pooling. To enable the model to first capture a larger temporal pattern and then proceed with capturing finer local patterns, the convolutional layers are formed with increasing filter sizes of 64, 128, and 256, and decreasing kernel sizes of 7,5 and 3, respectively. All convolutional layers have ReLU activation and same padding so that temporal dimensions are preserved

before pooling. One-dimensional MaxPooling layers with a pool size of 2 are used to down-sample the temporal resolution, and dropout layers with a rate of 0.3 are used after each convolutional block for regularizing training. After the last convolution layer, the feature maps are flattened and forwarded into a fully connected classification head that has two dense layers with 128 and 64 nodes and ReLU activation. The last output node employs a sigmoid activation for a binary ECG sequence classification of clean and tampered ECG sequences.
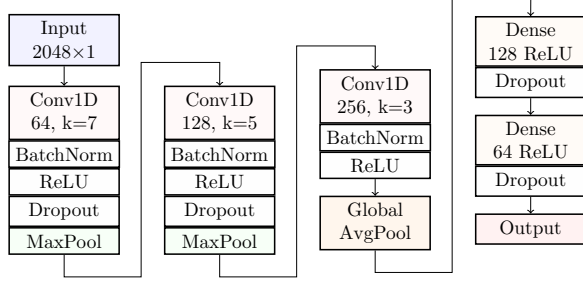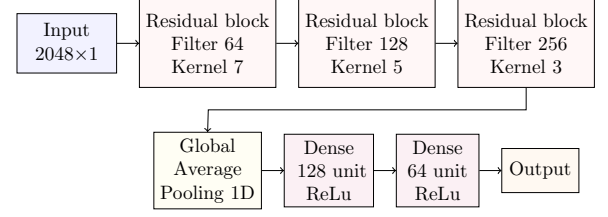

Fig. 12: 1D Convolutional Neural Network Model

(a) 1D ResNet Model

(b) Internal structure of the residual block used in the ResNet.

Fig. 13: Detailed view of the ResNet model architecture and its residual block design.

2) ResNet Model: The residual network (ResNet) architecture adopted in this study builds on the basic CNN design by adding residual connections, so that the model can learn deeper feature representations without suffering from the problem of gradient vanishing. The ResNet is made up of several stacked residual blocks that have two Conv1D layers with Batch normalization and ReLU activation functions. The residual connection skips over these two layers and is simply added to the block's output. After the residual blocks, the model uses a global average pooling layer to compact the temporal dimensions giving a fixed size feature vector regardless of the length of the input sequence. Such representation is then fed to a dense layer with a sigmoid activation function that does binary classification by classifying tampered and clean ECG segments. Stacking several residual blocks gives the ResNet the depth to extract hierarchical temporal features at different resolutions. This allows the model to identify tampering artifacts that can appear in various temporal scales from small waveform distortions to longer disruptions. With the help of residual learning, the architecture preserves high representational power with computational efficiency, which makes the architecture suitable for the tampering detection task on one-dimensional ECG inputs.

3) Transformer Model: Transformer-based architectures are a key focus of this work. Transformer-based models can learn temporal dependencies in long ECG segments and can therefore be highly effective at detecting ECG tampering compared to CNN models, where inconsistencies can be subtle and spread across multiple cardiac cycles. This section presents various transformer-based models used in this study.

i. Pure Transformer with Deep Feed-Forward Layers:

This model operates with ECG segments of shape 2048×96, which correspond to 4 s of ECG data in the time–frequency domain. Positional encoding is applied to the input to enable the model to learn key temporal placements of the waveforms
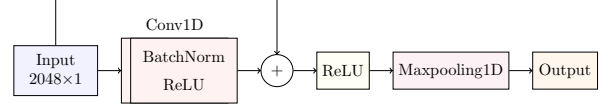
(P-wave, QRS complex, and T-wave), where morphology and timing are important for anomaly detection.

In this model, three stacked Transformer encoder blocks are selected to balance model complexity and generalization. Each encoder block has a multi-head attention block consisting of 8 attention heads, each of which has a subspace of 48 dimensions. Such a configuration allows the model to concentrate on several aspects of the ECG signal at once, including short-term variations and long-term dependencies of the waveform.

After the self-attention layer in every encoder block, a deep feed-forward network (FFN) is used to increase the representational ability of the model. Unlike the conventional two layer design, this FFN has three dense layers with a gradually reduced dimensionality, 384 units (4×96), 192 units (2×96), and 96 units. The first expansion to 384 units allows richer feature transformations, extracting complex interactions from the attention outputs. The stepwise decrease to 96 units filters and fine-tunes these features while preserving compatibility with residual connections, allowing stable training dynamics. GELU activations post the first two layers implement smoothing for fine-grained ECG fluctuations, and dropout layers after each dense operation reduce overfitting and enhance generalization to unobserved tampering patterns. A global average pooling operation is performed along the temporal dimension after the three transformer encoder blocks. This aggregation step creates a compact feature vector that summarizes the information over all 2048 time steps. Then two more dense layers of 512 and 256 units are used to further fine-tune the feature representation to produce the final classification output.
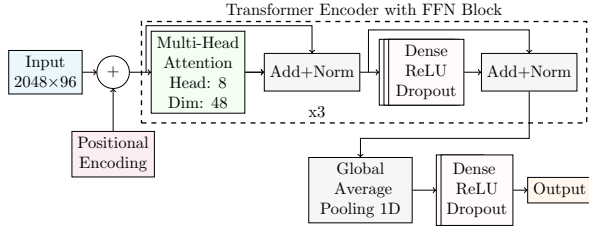
Fig. 14: Transformer Block with deep Feed-Forward Network and FFN classifier

ii. Transformer with CNN as Feed-Forward Layers:

This model is developed by replacing the feed-forward network (FFN) block in Fig. 14 with a CNN-based block. Except for this modification, the rest of the architecture positional encoding, multi-head attention, and global average pooling is consistent with the Transformer Block described above. The convolutional layers are constructed with successively reducing kernel sizes of 7, 5, and 3 and successively increasing filter sizes of 64, 128, and 96. By decreasing the kernel size along layers, the model constructs a hierarchy from coarse- to fine-grained temporal patterns. The more filters available on the convolutional layers, the more expressive the feature extraction can become with the increasing localization of the receptive field. Batch normalization is used after every convolutional operation to ensure that learning is stable. Dropout layers are also added after each convolution in order to avoid overfitting. This approach combines the strengths of local pattern extraction of CNNs and the long-range dependency learning capability of transformer models.
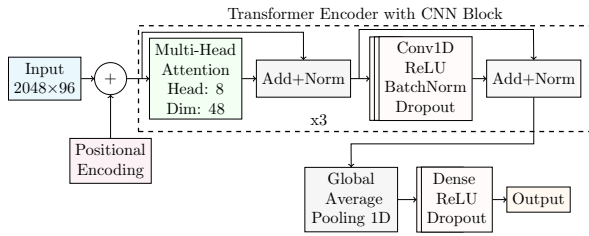

Fig. 15: Transformer block with CNN feed-forward layers and FFN classifier

iii. CNN as Feature Extractor + Transformer with deep FNN:

To achieve better tampering detection from raw one-dimensional ECG segments of shape 2048×1, a hybrid structure of convolutional feature extractor and Transformer encoder is proposed. The CNN model used to extract features is set up with step-down Kernel sizes at values of 13, 5, and 3 and with corresponding step-up filter depths of 64, 128 and 256 respectively. The use of a bigger kernel in the first layer enables the model to learn wide temporal trends that are then refined into localized morphological features by smaller kernels in subsequent layers. one-dimensional MaxPooling operations with pool size 2 are applied to decrease the temporal resolution and emphasize the dominant patterns,

while Batch Normalization and Dropout are applied all along to provide training stability and regularization. After feature extraction, the output is fed into sinusoidal positional encoding to restore the awareness of temporal order by the model. The encoded features are then passed through 3 Transformer encoder blocks, which are the same as the Transformer encoder blocks described in Fig. 14. This design enables the model to first convert the raw ECG signals into local feature representations and then globally reason over these features using the Transformer model. The results showed that it is possible to operate on one-dimensional ECG inputs directly and apply deep sequential modeling to achieve a significant enhancement of the detection of tampering artifacts.

iv. CNN Feature Extractor+Transformer with CNN Feed-Forward:

In this version, the input is raw 1D ECG segments of shape 2048×1. The CNN model used to extract features is similar to the CNN feature extractor used above, except the first kernel size is changed from 13 to 7. After the feature extraction and positional encoding, the features are fed to a Transformer encoder, which is the same as the Transformer encoder used in Fig. 15. The idea behind this architecture is to add hierarchical local feature refinement at various stages of the network: first at the raw signal level through the CNN feature extractor and then at the intermediate feature level through the CNN-augmented feed-forward stages of the Transformer. By the use of convolutional operations both before and within the Transformer blocks, the model is set to detect faint tampering signatures, which can either appear as localized irregularities in the waveform or as wider sequential discrepancies in the ECG signal.

v. CWT-based CNN Feature Extractor +Transformer:

This model is developed by extending the architecture shown in Fig. 14, a CNN module for feature extraction is incorporated and ECG signals with size 2048×96 is used as an input. The CNN feature extractor is constructed as three sequential Conv1D layers, where the filter depth increases (64, 128, and 256) and the kernel size decreases (7, 5, and 3). In this model, batch normalization, ReLU activations, and dropout layers are used to minimize overfitting, and one-dimensional MaxPooling layers are used to improve the extraction of key features. Then positional encoding is added to the feature sequence to model the sequential nature of the cardiac waveforms. The sequence is then sent through a set of Transformer encoder blocks. Unlike other architectures relying on deep feed-forward networks, this model uses a simple two-layer FFN in its Transformer block. This FFN first expands the feature dimension to 1024 units using a GELU activation and then projects it back to 256 units. Once the Transformer has processed the sequence of feature vectors, global average pooling is used to create a fixed-size feature vector. The feature vector is processed by two dense layers, each with 512 and 256 units, before being used to generate a binary output for detecting tampering. In comparison to other models, this model has two major differences: Firstly, the model uses CWT-transformed 2D ECG inputs rather than raw 1D signals;

secondly, it uses a regular Transformer encoder rather than deep or CNN-based FFNs. By using CNN feature extraction on the CWT spectrograms, the model can learn discriminative spatial patterns that are characteristic of anomalies. The Transformer encoder is responsible for modeling temporal relations between such features extracted so that detection of fine or distributed patterns of tampering that appear over time can be done.

B. Model Architecture for Person Verification

In this paper, a Siamese network architecture is used for person verification. The Siamese approach works by comparing two input sequences and drawing inferences related to their similarity. Each branch of the Siamese network operates on a single ECG input separately and identically, with every parameter being shared between the two branches so that embedding spaces are consistent. The network maps each input to a compressed latent form, to which a similarity score is calculated based on the distance between the two embeddings. Two encoders are studied under the Siamese framework, where each of them worked upon a different form of input data.
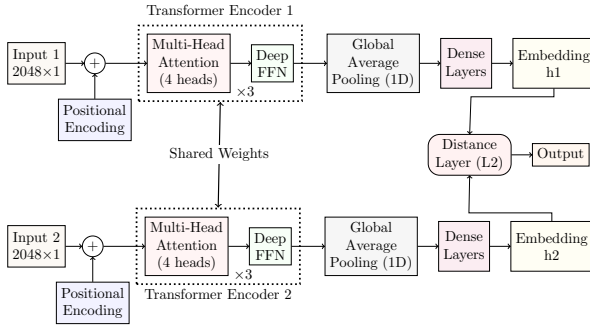

Fig. 16: Siamese Network Model Deep Transformer Encoder

1) Siamese Network with Deep Transformer Encoder: In the first variant, an ECG segment of shape 2048×96 is used as input, which corresponds to 4 s of the cardiac activity mapped into the time-frequency domain. The branch architecture adopts the deep Transformer encoder structure described earlier in Fig. 14, with the only change being the decrease of the number of attention heads from 8 to 4 in order to fit the scale of the verification task better, to a balance between expressive capacity and computational efficiency. The rest of the components, such as the multi-head self-attention mechanism, deep feed-forward network (FFN), residual connections, and positional encoding, are all in line with the original Transformer model.

2) Siamese Network with CNN Feature Extractor and Transformer Encoder: In the second version, all branches process raw one-dimensional ECG inputs of the form 2048×1. Hierarchical capture of localized morphological patterns is first obtained by a convolutional feature extractor; the extracted features are then fed to a Transformer encoder in a similar structure to the Transformer encoder discussed in Fig. 14. Empirical results verified that such a combination improves the person verification performance over a pure Transformer,

indicating that multi-level feature aggregation, i.e., local via CNNs and global via self-attention, offers a more discriminative embedding space for ECG-based identity verification.
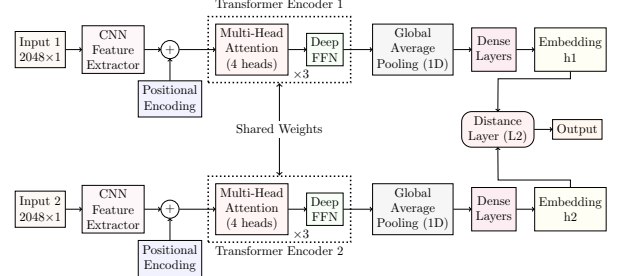

Fig. 17: Siamese Network with CNN Feature Extractor and Transformer Encoder

3) Training and Evaluation for Tampering Detection Models: All models were trained by using a balanced mix of tampered and untampered ECG signals, for each experiment, 50% of the sequences were clean, while the remaining 50% were tampered. The data were segmented into 4-second windows with 30% overlap to increase dataset density. To avoid artifacts from activity misalignment, tampering was performed only between segments representing the same physical activity (e.g., walking segments from one participant were replaced with walking segments from another). The experimental inputs consisted of either continuous wavelet transform for Transformer-based variants or raw 1D ECG signals for models where CNNs served as the initial feature extractor.

4) Training and Evaluation for Person Verification Model: The models for person verification were trained on pairs of ECG segments, with two balanced categories: positive pairs segment, segments formed from the same individual but different activities, and negative pairs segment, segments formed from different individuals performing the same activity. This pairing strategy enabled the model to learn identity features independent of activity variations. The input format used by the two model are different, the Siamese-Transformer model received CWT segments of size 2048×96, while the Siamese-CNN-Transformer model used raw 1D ECG signals of size 2048×1.

C. Computational Efficiency of Models

Floating Point Operations (FLOPs) measure the overall number of arithmetic operations (multiplications and additions) that are required by a model in a single forward pass. In this paper, as shown in table II, FLOPs are used to compare the computational burden of various tampering detection and person verification architectures quantitatively, so that the evaluation is not skewed towards accuracy but also the resource-efficiency and the implementation and deployment complexities of the models.

VI. EVALUATION

For tampering identification, seven models are proposed, and the performance of each deep learning model is evaluated

TABLE II: Model Computational Effort and Input Size

Model	Input Size	FLOPs (Millions)
CNN	2048×1	288
ResNet	2048×1	728
Tran-DeepFFN	2048×96 (CWT)	4646
Tran-CNNFFN	2048×96 (CWT)	3926
FeatCNN-Tran	2048×1	4277
FeatCNN-TranCNN	2048×1	4244
CWT-FeatCNN-Tran	2048×96 (CWT)	2179

across six tampering scenarios. For person identity verification, two Siamese network models are evaluated against different attacks. Stratified sampling is used to split the data collected into 80% training, 10% validation, and 10% testing sets. Each experiment is repeated 25 times, and the reported results represent the average accuracy over these runs.

A. Tampering Detection Results

This section presents the performance of the seven deep learning models for detecting ECG tampering. As shown in Table, III, all models performed well in the classification of heavily tampered signals, especially in the scenarios with sporadic 20% or 50% tampering, where detection accuracies varied from 91% to 98% respectively. The performance differences between the individual models became more apparent in more subtle cases such as 50:50 and 75:25 segment swaps. The models combining convolutional feature extraction with transformer encoding achieved some of the best results. Interestingly, ResNet was consistently competitive in all scenarios, though the transformer-based models exhibited the smallest performance variance across the 25 independent experiments. The CNN-based models exhibited significant performance fluctuations.

TABLE III: Detection Accuracy (%) for Different Tampering Strategies

Model	50-50	75-25	50-25(2)	50-10	Sp20	Sp50
Tran-Deep FFN	85.50	85.62	87.14	85.22	91.33	98.41
Tran-CNN FFN	86.50	85.80	87.30	92.10	91.62	98.91
FeatCNN-Tran	98.07	98.54	99.81	100	99.89	99.92
FeatCNN-TranCNN	98.46	98.68	99.78	100	99.83	99.94
CWT-FeatCNN-Tran	94.90	95.48	95.50	98.54	99.93	99.81
CNN	97.90	98.30	99.47	99.59	99.80	99.90
ResNet	98.10	98.78	98.36	100	99.90	100

Note: Sp20 = Sporadic 20%, Sp50 = Sporadic 50%, 50-10 = 50% A + 10% B alternating, 50-25(2) = 50% A + 25% B + 25% A, 50-50 = 50% A + 50% B, 75-25 = 75% A + 25% B.

To further gain insights about the performance of each model, the performance matrices were separately analyzed for each model and summarized in Tables IV through table IX. Table IV demonstrates that the 50-50 tampering was challenging for most models, while FeatCNN-TranCNN model obtained an accuracy of around 98.46%. Table V demonstrate that the 75–25 tampering scenario presented the subtle and smoothly blended changes, and the FeatCNN-TransCNN and FeatCNN-Trans models obtained the highest accuracies of 98.7% and 98.5%, respectively. The 50–25–25 tampering scenario involved a combination of medium-sized

segment replacements, and several models coped well with this tampering, as can be seen in table VI. For 50% Alternating tampering shown in table VII, the FeatCNN-Trans, FeatCNN-TransCNN and Resnet models had perfect detection performance, attaining 100% accuracy, precision, recall, and F1-score on all trials.

TABLE IV: Detailed Metrics (%) for 50-50 Tampering

Model	Accuracy	Precision	Recall	F1-Score
Tran-DeepFFN	85.48	84.29	86.69	85.47
Tran-CNNFFN	86.48	85.45	87.53	86.48
FeatCNN-Tran	98.07	98.02	98.13	98.07
FeatCNN-TranCNN	98.46	98.78	98.13	98.45
CWT-FeatCNN-Tran	94.88	94.35	95.41	94.88
CNN	97.90	97.73	98.05	97.90
ResNet	98.08	97.15	99.03	98.08

TABLE V: Detailed Metrics (%) for 75-25 Tampering

Model	Accuracy	Precision	Recall	F1-Score
Tran-DeepFFN	85.62	84.12	87.13	85.60
Tran-CNNFFN	85.80	84.74	86.87	85.79
FeatCNN-Tran	98.54	98.17	98.88	98.54
FeatCNN-TranCNN	98.68	98.46	98.90	98.68
CWT-FeatCNN-Tran	95.48	94.91	96.05	95.48
CNN	98.30	97.62	98.95	98.28
ResNet	98.78	98.50	99.05	98.78

TABLE VI: Detailed Metrics (%) for 50-25-25 Tampering

Model	Accuracy	Precision	Recall	F1-Score
Tran-DeepFFN	87.14	85.88	88.39	87.12
Tran-CNNFFN	87.30	86.59	87.98	87.28
FeatCNN-Tran	99.81	99.78	99.83	99.81
FeatCNN-TranCNN	99.78	99.81	99.78	99.78
CWT-FeatCNN-Tran	95.50	94.91	96.05	95.48
CNN	99.47	99.20	99.60	99.40
ResNet	98.36	97.77	98.95	98.36

TABLE VII: Detailed Metrics (%) for 50% Alternating Tampering

Model	Accuracy	Precision	Recall	F1-Score
Tran-DeepFFN	85.22	84.59	85.82	85.20
Tran-CNNFFN	92.10	91.49	92.67	92.08
FeatCNN-Tran	100.00	100.00	100.00	100.00
FeatCNN-TranCNN	100.00	100.00	100.00	100.00
CWT-FeatCNN-Tran	98.54	98.48	98.56	98.52
CNN	99.59	99.36	99.84	99.60
ResNet	100.00	100.00	100.00	100.00

TABLE VIII: Detailed Metrics (%) for Sporadic 20% Tampering

Model	Accuracy	Precision	Recall	F1-Score
CNN	99.80	99.84	99.76	99.80
ResNet	99.90	99.76	100.00	99.88
Tran-DeepFFN	91.33	90.70	91.87	91.28
Tran-CNNFFN	91.62	90.37	92.86	91.60
FeatCNN-Tran	99.89	100.00	99.78	99.89
FeatCNN-TranCNN	99.83	99.89	99.78	99.83
CWT-FeatCNN-Tran	99.36	99.12	99.44	99.28

TABLE IX: Detailed Metrics (%) for Sporadic 50% Tampering

Model	Accuracy	Precision	Recall	F1-Score
CNN	99.90	99.76	100.00	99.88
ResNet	100.00	100.00	100.00	100.00
Tran-DeepFFN	98.41	97.46	99.35	98.40
Tran-CNNFFN	98.91	98.33	99.44	98.88
FeatCNN-Tran	99.92	100.00	99.83	99.92
FeatCNN-TranCNN	99.94	100.00	99.89	99.94
CWT-FeatCNN-Tran	99.81	99.68	99.92	99.80

B. Person Specific Verification Results

Two types of Siamese models were developed for person identification, and the contrastive loss function is used to train the models. For variant 1, the Siamese Transformer ECG segment of shape 2048 × 96 is used, and for variant 2, the Siamese FeatureCNN-Transformer, one-dimensional ECG segments of the form 2048 × 1 is used. Pairing Strategy: Pairing strategy is conducted to make sure that the model learned person-specific characteristics rather than activity-specific patterns. As shown in table X ECG segments from the same individuals who perform different activities are used to form the positive pairs, and ECG segments from different individuals while performing the same activity are used to form the negative pairs.

TABLE X: Examples of Positive and Negative Pair

Pair Type	S 1 (Activity)	S2 (Activity)	Label
Positive Pair	S25 (Walking)	S25 (Sitting)	1
Negative Pair	S25 (Walking)	S36 (Walking)	0
Positive Pair	S40 (Cycling)	S40 (Running)	1
Negative Pair	S28 (Sitting)	S47 (Sitting)	0

The model is evaluated on an unseen test set consisting of similarly constructed positive and negative pairs and summarized in table XI.

TABLE XI: Detailed Metrics for Person Verification using Siamese Networks with Different Encoder Architectures

Encoder Used	Accuracy (%)	Precision (%)	Recall (%)	F1-Score (%)
Tran-DeepFFN	98.30	98.99	97.60	98.29
FeatCNN-Tran	100.00	100.00	100.00	100.00

C. Training Stability Observations

In a highly localized tampering scenario, CNN and ResNet model achieved high performance. However, they are sensitive to training parameter variations; their training result is not consistent, and minor variations in training configurations often resulted in significant performance differences. Therefore, they require careful hyperparameter tuning and stabilization to achieve consistent results.

D. Discussion

The experiment conducted demonstrate that FeatCNN-Tran, FeatCNN-TranCNN and ResNet models can effectively detect highly fragmented distortion introduced by tampering, even though such distortions are designed to mimic physiological or environmental noise. In particular, the intelligent tampering methods such 50%-50% and 75%-25% replacement, introduced subtle changes in time-domain and frequency-domain features, however this change were successfully identified by FeatCNN-TranCNN model with notable accuracy exceeding 98%.

Compared to prior studies that focus on detection of external adversarial manipulation and ECG based biometric identification, this study addresses less-explored yet critical challenge: the Intentional self-alteration and sophisticated modification of ECG signal for malicious purposes. In addition, the present work provides more advanced and robust tampering detection models by taking into account the strengths of different ML models. The study proposed improve the integrity and security of remote health monitoring systems. Table XII summarizes the body of work reviewed in section II and the study conducted in this article. The table highlights the importance of protecting the integrity of biomedical measurements. While many of the proposed approaches use publicly available datasets generated in controlled environments to develop and test their models, some rely on self-generated datasets created outside of clinical settings. Interestingly, the performance of these approaches is not inferior to those based on datasets created in controlled environments. Our approaches fall into the second category. However, our tamper emulation and detection models are significantly more robust. Furthermore, the data acquisition process involves more complex activities, which significantly impact the quality of the ECG measurements provided to the models. Nevertheless, the accuracy they achieved for tampering detection and person identification is better than the state of the art.

VII. CONCLUSIONS

This research evaluated the performance of CNN, ResNet, and hybrid deep learning architectures for ECG tampering detection, alongside a Siamese Transformer-based model for person-specific ECG verification. Experimental results show that in highly fragmented manipulation scenarios, CNN, FeatCNN-TranCNN, FeatCNN-Tran and ResNet models achieved above 99.5% accuracy; for subtle manipulations (e.g., 50%-50%) and (75%-25%) replacement, the FeatCNN-TranCNN models performed consistently better, achieving above 98% accuracy. The performance of CNN-based models (standard CNN and ResNet) is high in moderately tampered conditions; however, they exhibited high variability during training, indicating sensitivity to hyperparameters

TABLE XII: Compact comparison of ECG based biometric verification and tampering detection related studies

Work	Dataset	Environment	No. of subject	Model	Performance	Identification/tampering	Remarks
[24]	MIT-BIH, European ST-T, Holter	Clinical data set	47,N/A, N/A	HQCNN, CNN	Accuracy(%) HQCNN:94.3 CNN:92.5	yes/yes	Relies on quantum computing
[25]	PTBDB, CEBSDB	Public dataset	290, 20	MHT	EET: 7.62%	yes/yes	The MHT can be manipulated by changing user-specific keys
[26]	FECGSYN, ABFECGDB	Clinical dataset	10, 5	DAW-Net	F1 score of 98.13%	no/yes	Need accurate QRS localization
[27]	MIT-BIH, PTB	Public dataset	47, 290	CNN	Accuracy(%) PTB: 99.15; MIT-BIH :98.5	yes/no	Effective for stable heart rhythms
[28]	Fantasia, MITDB, ECG-ID, EDB, ADE	Public dataset	40, 47, 90, 79, 25	SAFD	Accuracy: 97.59%	yes/no	Sensitive to noise
[29]	MIT-BIH Arrhythmia, self-generated ECG dataset	Public dataset, un-controlled	47,30	SVD	Accuracy: 90%	yes/no	Existence of Linear correlation assumption
[30]	Self-generated ECG dataset	Uncontrolled	5	1D-CNN	Accuracy: 85%	yes/yes	Limited data set
[31]	Self-generated ECG dataset	Uncontrolled	34	CNN	Accuracy: >92%	yes/no	Data collected with 7 different activities
This work	Self-generated ECG dataset	Uncontrolled	54	ResNet, CNN, transformer+CNN	Accuracy: > 98%	yes/yes	Multiple tampering scenarios are considered

and a tendency toward overfitting. In contrast, the hybrid model (transformer-CNN) achieved high performance and also demonstrated more stable training across varying tampering levels. Pure Transformer models (Tran-DeepFFN) that work on CWT-transformed inputs performed relatively less well in terms of accuracies, particularly in cases of subtle tampering scenarios. Additionally, CWT-FeatCNN-Tran; where the inputs are first modified by CWT achieved moderate accuracies (about 95%-96%). It is also worth mentioning that CWT transformations also added additional computational overhead at the pre-processing step, and higher-dimensional CWT inputs (2048×96) increased model complexity and inference time. Hybrid designs that incorporated CNN components for feature extraction or into the Transformer feed-forward network performed better in terms of finding a balance between stability, computational efficiency, and peak accuracy. For person-specific ECG verification, the pure Transformer-Siamese network achieved an accuracy of 98.30%. In contrast, the hybrid CNN+Transformer-Siamese model delivered perfect verification performance with 100% accuracy. Future work will focus on incorporating more dataset to include varied patient profiles and integrating the model developed with edge computing platforms to enable real-time detection in wearable and mobile devices.

REFERENCES

[1] U. Satija, B. Ramkumar, and M. S. Manikandan, "Real-time signal quality-aware ecg telemetry system for iot-based health care monitoring," *IEEE Internet of Things Journal*, vol. 4, no. 3, pp. 815–823, 2017.

[2] M. B. Abubaker and B. Babayiğit, "Detection of cardiovascular diseases in ecg images using machine learning and deep learning methods," *IEEE Transactions on Artificial Intelligence*, vol. 4, no. 2, pp. 373–382, 2023.

[3] S. Ayeswarya and K. J. Singh, "A comprehensive review on secure biometric-based continuous authentication and user profiling," *IEEE Access*, vol. 12, pp. 82 996–83 021, 2024.

[4] N. Chakravarti and A. Singhal, "A comprehensive survey on infant biometric recognition," in *2025 2nd International Conference on Computational Intelligence, Communication Technology and Networking (CICTN)*, 2025, pp. 881–885.

[5] A. N. Uwaechia and D. A. Ramli, "A comprehensive survey on ecg signals as new biometric modality for human authentication: Recent advances and future challenges," *IEEE Access*, vol. 9, pp. 97 760–97 802, 2021.

[6] J. R. Pinto, J. S. Cardoso, and A. Lourenço, "Evolution, current challenges, and future possibilities in ecg biometrics," *IEEE Access*, vol. 6, pp. 34 746–34 776, 2018.

[7] S.-C. Wu, P.-L. Hung, and A. L. Swindlehurst, "Ecg biometric recognition: Unlinkability, irreversibility, and security," *IEEE Internet of Things Journal*, vol. 8, no. 1, pp. 487–500, 2021.

[8] S. Rahman, S. Pal, A. Habib, L. Pan, and C. Karmakar, "Attack-data independent defence mechanism against adversarial attacks on ecg signal," *Computer Networks*, vol. 258, p. 111027, 2025.

[9] S.-M. Moosavi-Dezfooli, A. Fawzi, O. Fawzi, and P. Frossard, "Universal adversarial perturbations," pp. 1765–1773, 2017.

[10] S. Ahmed and S. H. Cho, "Machine learning for healthcare radars: Recent progresses in human vital sign measurement and activity recognition," *IEEE Communications Surveys and Tutorials*, vol. 26, no. 1, pp. 461–495, 2024.

[11] C. Tan, L. Zhang, T. Qian, S. Brás, and A. J. Pinho, "Statistical n-best afd-based sparse representation for ecg biometric identification," *IEEE Transactions on Instrumentation and Measurement*, vol. 70, pp. 1–13, 2021.

[12] X. Tang, S. Liu, W. Che, and W. Tang, "Tampering attack detection in analog to feature converter for wearable biosensor," in *2022 IEEE International Symposium on Circuits and Systems (ISCAS)*, 2022, pp. 1150–1154.

[13] K. Nezamabadi, N. Sardaripour, B. Haghi, and M. Forouzanfar, "Unsupervised ecg analysis: A review," *IEEE Reviews in Biomedical Engineering*, vol. 16, pp. 208–224, 2023.

[14] H.-S. Choi, B. Lee, and S. Yoon, "Biometric authentication using noisy electrocardiograms acquired by mobile sensors," *IEEE access*, vol. 4, pp. 1266–1273, 2016.

[15] Y. Chu, H. Shen, and K. Huang, "Ecg authentication method based on parallel multi-scale one-dimensional residual network with center and margin loss," *IEEE Access*, vol. 7, pp. 51 598–51 607, 2019.

[16] L. S. Watson and A. Anitha, "Comparative analysis of machine learning and deep learning models for high-precisior classification in cyberattack detection," in *2024 9th International Conference on Communication and Electronics Systems (ICCES)*, 2024, pp. 1663–1671.

[17] S. S. Abdeldayem and T. Bourlai, "A novel approach for ecg-based human identification using spectral correlation and deep learning," *IEEE Transactions on Biometrics, Behavior, and Identity Science*, vol. 2, no. 1, pp. 1–14, 2020.

[18] R. N. A. Begum, A. Sharma, and G. K. Singh, "An ensemble model of dl for ecg-based human identification," *IEEE Transactions on Instrumentation and Measurement*, vol. 73, pp. 1–15, 2024.

[19] Z. Li, F. Liu, W. Yang, S. Peng, and J. Zhou, "A survey of convolutional neural networks: Analysis, applications, and prospects," *IEEE Transactions on Neural Networks and Learning Systems*, vol. 33, no. 12, pp. 6999–7019, 2022.

[20] P. G. Aublin, J. Felblinger, and J. Oster, "A generalisable heartbeat classifier leveraging self-supervised learning for ecg analysis during magnetic resonance imaging," *IEEE Journal of Biomedical and Health Informatics*, vol. 28, no. 9, pp. 5147–5155, 2024.

[21] T. Gao, X. Xie, H. Liu, S. Zhou, and M. Shu, "A multilevel metric fusion framework for few-shot electrocardiogram classification," *IEEE Transactions on Instrumentation and Measurement*, vol. 74, pp. 1–11, 2025.

[22] M. J. Baucas, P. Spachos, and S. Gregori, "Internet-of-things devices and assistive technologies for health care: Applications, challenges, and opportunities," *IEEE Signal Processing Magazine*, vol. 38, no. 4, pp. 65–77, 2021.

[23] D. Le, S. Truong, P. Brijesh, D. A. Adjeroh, and N. Le, "scl-st: Supervised contrastive learning with semantic transformations for multiple lead ecg arrhythmia classification," *IEEE Journal of Biomedical and Health Informatics*, vol. 27, no. 6, pp. 2818–2828, 2023.

[24] Z. Qu, W. Shi, B. Liu, D. Gupta, and P. Tiwari, "Iomt-based smart healthcare detection system driven by quantum blockchain and quantum neural network," *IEEE journal of biomedical and health informatics*, vol. 28, no. 6, pp. 3317–3328, 2023.

[25] W. Yang and S. Wang, "A privacy-preserving ecg-based authentication system for securing wireless body sensor networks," *IEEE Internet of Things Journal*, vol. 9, no. 8, pp. 6148–6158, 2021.

[26] B. Samuel and M. K. Hota, "Dual attention based pipelined encoder-decoder network for fetal electrocardiogram extraction," *IEEE Transactions on Instrumentation and Measurement*, 2025.

[27] G. Wang, S. Shanker, A. Nag, Y. Lian, and D. John, "Ecg biometric authentication using self-supervised learning for iot edge sensors," *IEEE Journal of Biomedical and Health Informatics*, 2024.

[28] T. Qian, L. Zhang, and Z. Li, "Algorithm of adaptive fourier decomposition," *IEEE Transactions on Signal Processing*, vol. 59, no. 12, pp. 5899–5906, 2011.

[29] P. Huang, L. Guo, M. Li, and Y. Fang, "Practical privacy-preserving ecg-based authentication for iot-based healthcare," *IEEE Internet of Things Journal*, vol. 6, no. 5, pp. 9200–9210, 2019.

[30] M. Usman, M. Kamal, and M. Tariq, "Improved and secured electromyography in the internet of health things," *IEEE journal of biomedical and health informatics*, vol. 26, no. 5, pp. 2032–2040, 2021.

[31] W. Dargie, S. Farrokhi, and C. Poellabauer, "Identification of persons based on electrocardiogram and motion data," *IEEE Sensors Journal*, 2025.